Direct Derivation of the Free Energy of Two Charged Lamellar Colloids from (*N*,*V*,*T*) Monte Carlo Simulations

A. Delville* and P. Levitz

CRMD, CNRS 1B rue de la Férollerie, 45071 Orléans Cedex 02, France

Received: July 24, 2000; In Final Form: October 2, 2000

We used (*N*,*V*,*T*) Monte Carlo simulations to calculate the configurational entropy and the free energy of two charged disks neutralized by mono- and divalent counterions. All ion−ion, ion−disk, and disk−disk interactions are described in the framework of the Primitive model. This treatment includes interionic correlations responsible for long-range attraction between colloids under high electrostatic coupling conditions. The free energy is fitted by an empirical law which may be used for numerical simulation of colloidal suspensions in the framework of the One Component Plasma theory, including electrostatic and excluded volume effects.

I. Introduction

Charged colloids display a large variety of physicochemical properties (swelling, adhesion, aggregation, adsorption, ...) used in many industrial applications. Electrostatic interactions have been studied for various materials (spherical latex or micelles; fibrous DNA, tobacco virus or polyelectrolytes; clays or cement lamellae). They are responsible for the long-range coupling between such colloidal particles and govern their macroscopic behavior. In that context, much effort[1−3] has been devoted to the description of the diffuse layers of counterions trapped in the electrostatic well in the vicinity of the charged colloids (the so-called condensed counterions) because they modulate the electrostatic coupling between the colloids.

The purpose of this study is to derive the free energy of colloidal suspensions of charged lamellar colloids from a Monte Carlo description of their clouds of condensed counterions. Suspensions of charged lamellae has been the subject of recent experimental investigations,[4−18] showing the relationship between structural and mechanical properties of these strongly coupled systems. There is a need of rationalization taking into account both electrostatic[5,19−25] and excluded volume[26,27] effects between nonspherical charged colloids. The structural and mechanical properties of suspensions of such colloids are still not fully understood. As an example, the equation of state of Laponite clay in the presence of salt[5−6,13] displays a plateau corresponding to a gas−liquid transition. Furthermore, SAXS spectra of diluted salt free suspensions of Laponite[18] exhibit a correlation peak corresponding to interparticle separation *larger* then the average separation between the clay particles. Both observations are due to an effective attraction between the clay particles while the equation of state of clay suspensions yields a strongly repulsive force. The general purpose of this study is to derive the effective pair potential describing the interactions between two Laponite particles, by taking explicitly into account the electric charges and the shape of these clay particles. The structural and mechanical properties of suspensions of such nonspherical charged colloids result from the competition between two antagonistic effects: electrostatic interactions and excluded volume effects. The later have been shown to align neighboring lamellae parallel to each other[26,27] while electrostatic contributions are optimized by a perpendicular orientation[5,21] of charged disks. The effective pair potential obtained by the present study includes both effects.

* Corresponding author. E-mail: delville,levitz@cnrs-orleans.fr.

The conclusions of these simulations should at least elucidate the origin of the effective attraction reported above, which may originate from the mean force potential describing the effective interaction between a single pair of particles or from multiple-body interactions. Furthermore, our effective pair potential will be useful for an empirical description of colloidal suspensions performed in the framework of the one-component plasma (OCP) approach,[25,28] taking into account the contribution of the anisotropic[20,22−24] diffuse layers surrounding these nonspherical particles better than a Yukawa potential.[25]

This treatment is performed in the framework of the primitive model. It includes interionic correlations responsible for the cohesion of highly coupled colloids.[29] These correlations are neglected in classical treatments of the diffuse layer based on numerical solution of the Poisson−Boltzmann equation. The only assumption implied in this study is the additivity of the effective pair potential in order to describe the interactions between many colloids[30] within colloidal suspensions.

II. Methods

(A) Calculation of Energy and Forces. Two hard disks (diameter 300 Å, thickness 10 Å) are maintained parallel to each other and located at the center of a large simulation cell (width 1500 Å). Each disk bears 1020 negative sites distributed within a regular network in the equatorial plane of the disk. These parameters describe the apparent size and net electric charge of Laponite clay particles[31,32] used in numerous experimental studies.[4−18] Laponite is a trioctahedral clay obtained by sandwiching one layer of octahedral magnesium oxide between two layers of tetrahedral silicium oxide. The electric charge of Laponite results from the substitution of some magnesium cations of the octahedral layer by lithium cations. At the pH conditions of our experimental studies,[5−6,11,13,18] the dangling bonds at the edges of the particles are saturated by protons, and no electric charge is detected.[31] Thus, as far as long-range electrostatic couplings are concerned, the Laponite particle may be modeled by a rigid disk limited by two repulsive planes of finite length. The negative charges are localized uniformly in the equatorial plane of the disk as this corresponds to the location the lithium cations within the octahedral layer. These negative charges of the clays are neutralized by mono- or divalent counterions (diameter 4.5 Å), mimicking hydrated sodium or calcium cations. Figure 1 displays a snapshot of one equilibrium configuration of condensed monovalent counterions.

10.1021/jp002625p CCC: $20.00
Published on Web 12/29/2000

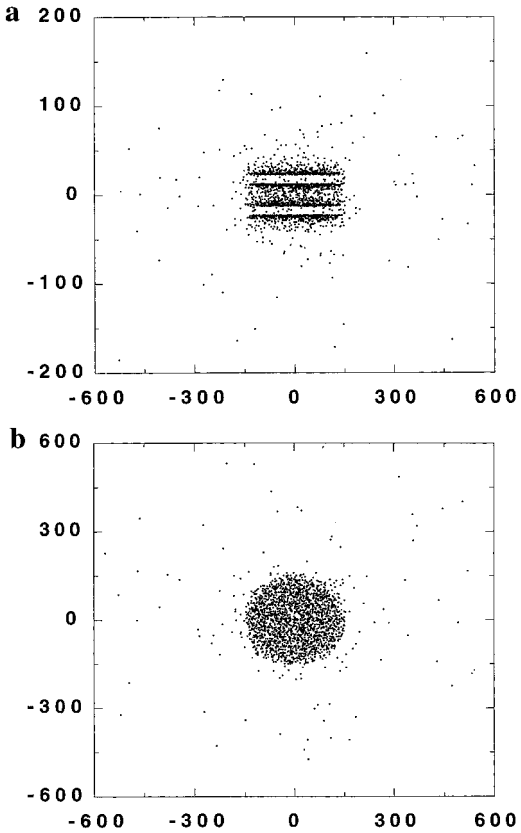

Figure 1. Lateral (a) and vertical (b) views of a snapshot illustrating the equilibrium configuration of monovalent counterions condensed in the vicinity of two parallel charged disks with a center/center separation of 35 Å.

Ion−ion, ion−site, and site−site electrostatic interactions are described in the framework of the primitive model:

$$u_{ij}(r_{ij}) = \frac{q_i q_j}{4\pi e_0 \epsilon_r r_{ij}} \qquad \text{if } r_{ij} \geq a_{ij} \tag{1a}$$

$$u_{ij}(r_{ij}) = \infty \qquad \text{otherwise} \tag{1b}$$

where a_{ij} is the ion diameter. The dielectric constant of the solvent (ϵ_r) is set equal to 78.5 to describe bulk water. The electrostatic energy is calculated using Ewald summation with classical 3D minimum image convention and periodic boundary conditions

$$E_{elect} = E_{dir} + E_{self} + E_{mom} + E_{rec} \tag{2a}$$

$$E_{dir} = \frac{0.5}{4\pi\epsilon_0\epsilon_r}\sum_{i=1}^{N_i} q_i \sum_{j=1,i\neq j}^{N_j} \frac{q_j \,\mathrm{erfc}(\kappa r_{ij})}{r_{ij}} \tag{2b}$$

$$E_{self} = -\frac{\kappa}{4\pi^{3/2}\epsilon_0\epsilon_r}\sum_{i=1}^{N_i} q_i^2 \tag{2c}$$

$$E_{mom} = \frac{2\pi}{V(1+e_\infty)4\pi\epsilon_0\epsilon_r}\{\sum_{i=1}^{N_i} q_i \mathbf{r}_i\} \tag{2d}$$

$$E_{rec} = \frac{2\pi}{V4\pi\epsilon_0\epsilon_{r|\mathbf{K}|\neq 0}} \sum \frac{\exp(-\mathbf{K}^2/4K^2)}{\mathbf{K}^2} \cdot [\{\sum_{i=1}^{N_i} q_i \cos(\mathbf{K}\mathbf{r}_i)\}^2 + \{\sum_{i=1}^{N_i} q_i \sin(\mathbf{K}\mathbf{r}_i)\}^2] \tag{2e}$$

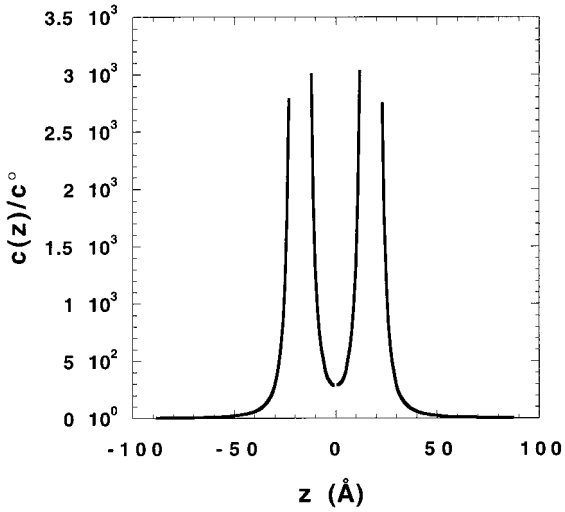

Figure 2. Lateral view of the local concentration profile of monovalent counterions averaged over the cross section of the two disks under the same condition as in Figure 1.

where e_∞, the dielectric constant of the continuum surrounding the replica of the simulation cell, is set equal to 1. The screening parameter κ is set to 3.3×10^{-3} Å^{-1} and the summation over the reciprocal space is cut for $|\mathbf{K}| \geq 5 \cdot 2\pi/L$, where L is the length of the simulation cell. Since this length is 1500 Å, the limitation on the summation in the reciprocal space leads to an accuracy better than 2×10^{-3} for the electrostatic energy.[33]

In addition to this electrostatic component, the total interaction between the two disks includes van der Waals attraction. The van der Waals component is described as the sum of interactions between two sets of elementary cubes, with a volume (noted V_{cell}) equal to 10^3 Å^3 and centered on the 1020 charged sites of each disk. The van der Waals energy is given by

$$E_{vdw} = -\frac{HV_{cell}^2}{\pi^2}\sum_{i=1}^{Ns}\sum_{j=1}^{Ns} r_{ij}^{-6} \tag{3}$$

where the Hamaker constant ($H = 2.2 \times 10^{-20}$ J)[34] describes the van der Waals attraction between two mica particles dispersed in water.

The net force acting on each disk results from the sum of the disk−disk and disk-ion forces calculated from the derivation of the electrostatic (eq 2) and van der Waals (eq 3) potentials. In addition to these long-range forces we also include the contribution from the contact force exerted on each particle by the condensed counterions in contact with the two basal surfaces of the disks. The net contact force results, thus, from a balance between the fraction of counterions condensed on the inner and outer faces of each disk (see Figure 2):

$$F_{contact} = kT\sigma\{c(\mathrm{cont})_{inner} - c(\mathrm{cont})_{outer}\} \tag{4}$$

where σ is the cross section of the disk and c(cont) is the local concentration of ions in contact with the inner or outer basal surfaces of the disks. Because of the overlap of the electrostatic wells located in the vicinity of each surface, more counterions are condensed in the interparticle domain,[23] leading always to a net repulsive contribution of the ion−disk contact force.

(B) Calculation of the Entropy. To derive the free energy of the colloidal suspension as a function of the separation between the two parallel charged disks, we further calculate the entropy characterizing the equilibrium configurations of the counterions ($\{n_j\}$). For that purpose, the total volume of the

simulation cell (V) is divided into M elementary volumes (noted v_j), each containing n_j counterions. The entropy is then evaluated by using

$$S = k \ln P_S(\{n_j\}) \tag{5a}$$

$$\ln P_S(\{n_j\}) = \sum_{j=1}^{M} n_j \ln \frac{N^\circ v_j}{n_j V} \tag{5b}$$

where N° is the total number of counterions in the simulation cell. Equations 5a,b result from a digitalization of the mixing entropy of the counterions[28]

$$S = -k \int d\mathbf{r}\, \rho(\mathbf{r})\{\ln[\rho(\mathbf{r})/\rho^\circ] - 1\} \tag{6}$$

where $\rho(\mathbf{r})$ is the local density of counterions and ρ° its average value. In the framework of the density functional theory,[1−2,35−38] the free energy of the counterions may always be separated into ideal, external, interionic, and correlation parts:

$$F = F^{id} + F^{ext} + F^{cc} + F^{corr} \tag{7a}$$

$$F^{id} = kT \int d\mathbf{r}\, \rho(\mathbf{r})\{\ln[\rho(\mathbf{r})\Lambda^3] - 1\} \tag{7b}$$

$$F^{ext} = \sum_p \int d\mathbf{r}\, \rho(\mathbf{r})\, V_p(r) \tag{7c}$$

$$F^{cc} = \frac{q^2}{4\pi\epsilon_0\epsilon_r} \int\int d\mathbf{r}\, d\mathbf{r}' \frac{\rho(\mathbf{r})\, \rho(\mathbf{r}')}{|\mathbf{r} - \mathbf{r}'|} \tag{7d}$$

where Λ is the Debye length of the counterions and V_p is the electrostatic potential generated by the clay particle noted p. Finally F^{corr} includes the interionic correlations resulting from ion−ion electrostatic and excluded volume potentials. If all energetic contributions are neglected (ideal gas), F reduces to F^{id} which differs from the mixing entropy (eq 6) by an additive constant. Note that our Monte Carlo simulations include implicitly the contribution from the interionic correlations in the derivation of the entropic (eq 7b) and energetic (eqs 7) parts of the free energy.

Four sets of nonoverlapping elementary volumes are used to evaluate the mixing entropy of the counterions whose concentration varies sharply near the disk surfaces (see Figure 2) because of ionic condensation. To describe the structure of the first shell of counterions condensed at the surface of the disks, the first set of elementary volumes is composed of 20 layers (thickness 0.5 Å) of one hundred angular sectors mapping the basal surfaces of each disk. The second set of elementary volumes is a regular network of 8000 cubes (length 50 Å) forming a large cube (length 1000 Å) at the center of the simulation cell. The third set of elementary volumes is composed of 10 concentric spherical shells with radii varying between 500 Å (one-half of the global cube length of the second set) and 750 Å (one-half of the simulation cell length). The final set is composed of the eight residual corners of the simulation cell cut by the last shell of the third set of elementary volumes. The volume fraction of each cube of the second set of elementary volumes overlapping with elementary volumes of the first and third sets are evaluated by preliminary Monte Carlo sampling. This evaluation of the mixing entropy is accurate enough, since increasing the number of elementary volumes by a factor of 2 modifies the entropy variation by less than one percent.

Monte Carlo simulations are performed in the (N,V,T) ensemble by using the classical Metropolis sampling procedure, with block averages to reduce statistical noise. The size of the blocks is at least equal to 10 times the total number of ions. All simulations were performed for 298 K.

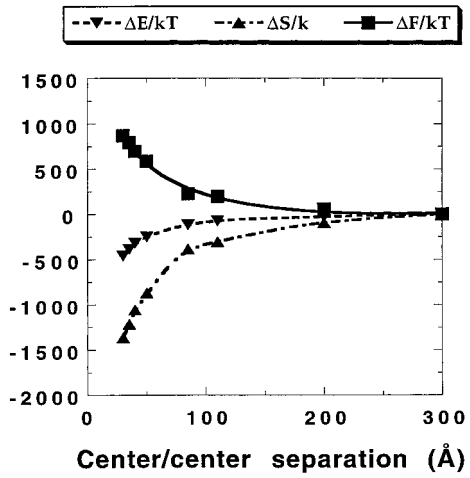

Figure 3. Variation of the free energy (■), total energy (▲), and mixing entropy (▼) for parallel charged disks neutralized by monovalent counterions.

III. Results and Discussion

(A) Monovalent Counterions. The variation of the total free energy as a function of the disk separation is drawn in Figure 3 along with its energetic and entropic contributions. The electric charges of the disks are neutralized by 2040 monovalent counterions and no salt is added to the solution. As already stated,[23,29] the electrostatic energy is negative and decreases continuously when the disk separation is reduced. The electrostatic coupling *alone* would cause the collapse of such charged colloids, because the ion-colloid attraction overcomes the ion−ion and colloid-colloid repulsions. However, the free energy is repulsive due to the overcoming entropy contribution which also decreases when the disk separation is reduced. This last result was expected intuitively since the overlap of the diffuse layers, and thus the departure from completely random ionic distribution, increases when the disk separation is reduced.

The variation of the free energy as a function of the disk separation D (expressed in Å) may be fitted by a simple mathematical law

$$\Delta F(D) = kT\left\{(2.3 \pm 0.5)D + (580 \pm 90) \ln\left[\frac{90 \pm 5}{D - (8 \pm 5)}\right]\right\} \tag{8}$$

This empirical law has no physical basis, but it contains all the physical information required to describe the mechanical behavior (swelling) of these charged nonspherical colloids. It was obtained by generalized least-squares fitting and leads to a root-mean-squared deviation of 0.9965 (for 8 points). The 95% confidence limits are also given for each parameter in eq 8.

This equation may be useful for simple treatments of suspensions of such charged lamellar colloids in the framework of the OCP theory:[25] it includes all contributions from ion−ion and ion-colloid interactions and differs somewhat from the classical Yukawa's law,[25,28] frequently used in such studies. Obviously, this effective potential is valid only for two parallel charged disks and further calculations must be performed for other relative orientations of the two disks in order to allow the simulation of a disordered system.

To check our derivation of the free energy, we have also compared the direct calculation of the longitudinal component of the force acting on each disk to an analytical derivation of

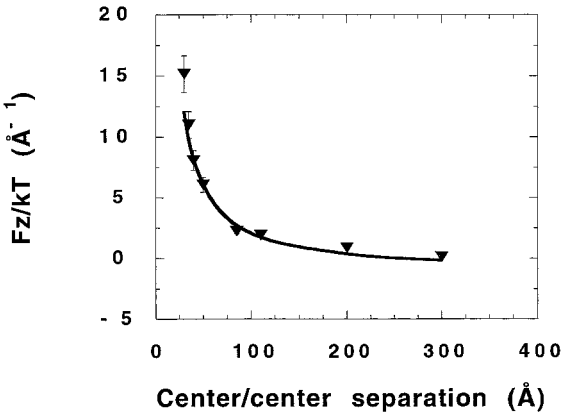

Figure 4. Net force acting on the disk determined from the equilibrium configurations of the monovalent counterions (▼) or analytically derived from the free energy variation (—, see text).

the empirical free energy (eq 8) divided by two, since the free energy is an extensive thermodynamical property:

$$F_z/kT = -\frac{1}{2kT}\frac{\partial \Delta F(D)}{\partial D} = -(1.15 \pm 0.25) + \frac{(290 \pm 45)}{D - (8 \pm 5)} \quad (9)$$

Both derivations are shown in Figure 4, leading to a satisfactory agreement within the whole range of interparticle separations. The analytical derivation (eq 9) slightly underestimates the net force at the smallest separation only. This result validates our direct calculation of the entropy and thus the free energy of the suspension.

The net contribution of the van der Waals attraction to the free energy is negligible (i.e., less than 0.02 *kT*) at center-to-center separations larger than 50 Å. The largest van der Waals attraction is obviously reported at the smallest separation but its contributions to the total force (−2.3 *kT*/Å) and energy (−14 *kT*) remain respectively one or 2 orders of magnitude smaller than the sum of the electrostatic and contact contributions (see Figures 3 and 4). As a consequence, modifying the Hamaker constant (eq 3) by 20% will have no influence on the simulation results.

(B) Divalent Counterions. When the electrostatic coupling between charged colloids increases, for example by increasing the charge of the counterions, the interparticle repulsion disappears due to the enhancement of interionic correlations.[29] As shown in Figure 5, the detailed balance between electrostatic attraction and entropic repulsion differs totally from the results obtained previously with monovalent counterions (see Figure 3) since both electrostatic and entropic contributions have in this case the same order of magnitude. As a consequence the variation of the total free energy is almost zero (as compared to the statistical uncertainty), except at the smallest separation. This result is in qualitative agreement with the calculation of the net force acting on the disks (Figure 6). Because of the reduced order of magnitude of the results displayed in Figures 5 and 6, they appears highly noisy and even not significant; however the absolute value of the errors affecting these data has the same order of magnitude as in the case of monovalent counterions.

(C) Effect of Salt. A third set of simulations is performed for two disks neutralized by monovalent counterions and at a center to center separation of 20 Å in the presence of salt. At such separation, the net repulsion between disks neutralized by monovalent counterions was shown to originate from the contact force.[23] Both electrostatic and van der Waals forces remain

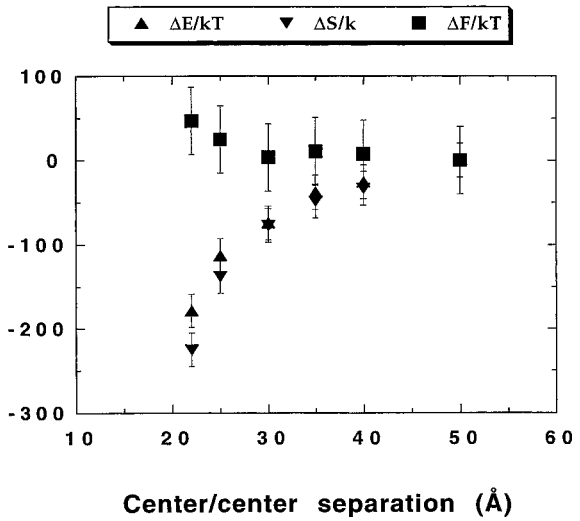

Figure 5. Variation of the free energy (■), total energy (▲), and mixing entropy (▼) for parallel charged disks neutralized by divalent counterions.

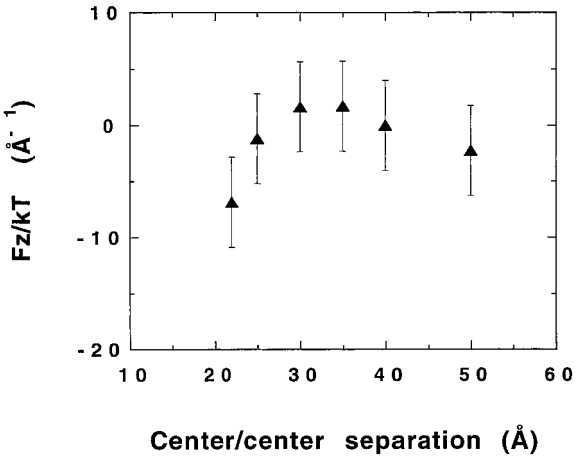

Figure 6. Net force acting on the disk determined from the equilibrium configurations of the divalent counterions.

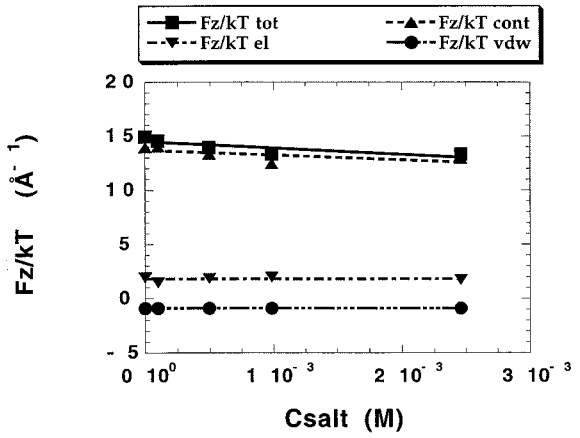

Figure 7. Influence of the concentration of salt of monovalent ions on the net force acting on the disks and its different contributions: (■) total force; (▼) electrostatic contribution; (▲) contact force; (●) van der Waals contribution.

negligible, and the net force acting on the disk results from the balance between the contact force exerted by the counterions at contact with the inner and outer surfaces of the disks (see Figure 7).

We thus wondered about the influence of added salt, whose counterions may further accumulate in the interparticle domain,

enhancing the contact repulsion exerted on the disks. This result would be in contradiction with the decrease of the osmotic compression generally reported for infinite lamellae in the presence of added salt.[34,39] As shown in Figure 7, this disagreement is not detected: the electrostatic and van der Waals forces are insensitive to the added salt, and the contact pressure is slightly reduced when salt is added to the suspension, leading to a simultaneous reduction of the net repulsion between the disks. Excluded volume effects between the dense layers of counterions condensed at the inner surface of the disks restrict the increase of the number of counterions in the interparticle domain when salt is added to the solution. In that context, it might be interesting to further investigate the influence of the ionic diameter on the stability of finite colloids. Ion−ion contact repulsion was shown to increase the net repulsion between infinite charged lamellae,[29] but is also expected to reduce the amount of counterions confined between the two disks and condensed in contact with the inner surfaces of the disks. Therefore, further simulations are required to determine which of these antagonistic effects will drive the swelling behavior of finite charged disks neutralized by monovalent counterions.

(D) Limitations and Outlook. To our knowledge, this result is the first direct derivation of the free energy of suspensions of charged colloids performed from ionic equilibrium distributions obtained from Monte Carlo simulations. The free energy of colloidal suspensions was generally derived from an integration of the net interparticle force or pressure[40,41] as a function of the interparticle separation. However, the resulting accumulation of statistical uncertainties generally leads to noisy results.

Our derivation of the free energy includes implicitly contributions from interionic correlations, responsible for attractions between highly coupled colloids. The resulting empirical law describing the variation of the free energy as a function of the disk separation will be of great interest for modeling colloidal suspensions in the framework of the OCP theory.[25]

We are currently further investigating the influences of the relative orientation of the disks and of the amount of added salt to their mutual repulsion. The purpose of this study is to better understand the complexity of the phase diagram displayed by colloidal suspensions of such anisotropic charged particles and elucidate the appearance of some effective attraction between nonspherical charged colloids.

Obviously, the validity of this approach is restricted by the assumption of the additivity of the effective pair potential describing the distribution of the colloids. Quantifying the influence of long-range coupling between many particles[30] will be the subject of our further research in that field.

IV. Conclusion

By calculating the total energy and the mixing entropy of the ionic distribution around two parallel charged disks we obtain a direct derivation of the free energy of lamellar colloids. The free energy is then fitted by an empirical analytical law, useful for statistical treatments of such colloidal suspensions in the framework of the OCP theory. By contrast with the classical Yukawa potential, this effective pair potential includes all contributions from electrostatic and excluded volume effects such as interionic correlations.

Acknowledgment. We cordially thank Dr. R. Setton (CRMD, Orleans, France) for interesting discussions. Monte Carlo simulations were performed locally on workstations purchased thanks to grants from Région Centre (France) and COMI (CNRS, France), on workstations from the Gage Laboratory (Palaiseau, France) and on Nec Supercomputer (IDRIS, Orsay, France).

References and Notes

(1) Löwen, H. *Phys. Rep.* **1994**, *237*, 249.
(2) Attard, Ph. *Adv. Chem. Phys.* **1996**, *92*, 1.
(3) Ninham, B. W. *Adv. Colloid Interface Sci.* **1999**, *83*, 1.
(4) Ramsay, J. D. F.; Lindner, P. *J. Chem. Soc., Faraday Trans.* **1993**, *89*, 4207.
(5) Mourchid, A.; Delville, A.; Lambard, J.; Lécolier, E.; Levitz, P. *Langmuir* **1995**, *11*, 1942.
(6) Mourchid, A.; Delville, A.; Levitz, P. *Faraday Discuss.* **1995**, *101*, 275.
(7) Pignon, F.; Piau, J. M.; Magnin, A. *Phys. Rev. Lett.* **1996**, *76*, 4857.
(8) Gabriel, J. C. P.; Sanchez, C.; Davidson, P. *J. Phys. Chem.* **1996**, *100*, 11139.
(9) Kroon, M.; Wegdam, G. H.; Sprik, R. *Phys. Rev. E* **1996**, *54*, 6541.
(10) Pignon, F.; Magnin, A.; Piau, J. M.; Cabane, B.; Lindner, P.; Diat, O. *Phys. Rev. E* **1997**, *56*, 3281.
(11) Mourchid, A.; Levitz, P. *Phys. Rev. E* **1998**, *57*, R4887.
(12) Kroon, M.; Vos, W. L.; Wegdam, G. H. *Phys. Rev. E* **1998**, *57*, 1962.
(13) Mourchid, A.; Lécolier, E.; Van Damme, H.; Levitz, P. *Langmuir* **1998**, *14*, 4718.
(14) van der Krooij, F. M.; Lekkerkerker, H. N. W. *J. Phys. Chem. B* **1998**, *102*, 7829.
(15) Bonn, D.; Tanaka, H.; Wegdam, G.; Kellay, H.; Meunier, J. *Europhys. Lett.* **1998**, *45*, 52.
(16) Saunders, J. M.; Goodwin, J. W.; Richardson, R. M.; Vincent, B. *J. Phys. Chem B* **1999**, *103*, 9211.
(17) Bonn, D.; Kellay, H.; Tanaka, H.; Wegdam, G.; Meunier, J. *Langmuir* **199**, *15*, 7534.
(18) Levitz, P.; Lécolier, E.; Mourchid, A.; Delville, A.; Lyonnard, S. *Europhys. Lett.* **2000**, *49*, 672.
(19) Forsyth, P. A.; Marcelja, S.; Mitchell, D. J.; Ninham, B. W. *Adv. Colloid Interface Sci.* **1978**, *9*, 37.
(20) Chang, F. R. Ch.; Sposito, G. *J. Colloid Interface Sci.* **1996**, *178*, 555.
(21) Dijkstra, M.; Hansen, J. P.; Madden, P. A. *Phys. Rev. E* **1997**, *55*, 3044.
(22) Hsu, J. P.; Tseng, M. T. *Langmuir* **1997**, *13*, 1810.
(23) Delville, A. *J. Phys. Chem. B* **1999**, *103*, 8296.
(24) Leote de Carvalho, R. J. F.; Trizac, E.; Hansen, J. P. *Phys. Rev. E* **2000**, *61*, 1634.
(25) Kutter, S.; Hansen, J. P.; Sprik, M.; Boek, E. *J. Chem. Phys.* **2000**, *112*, 311.
(26) Onsager, L. *Ann. N. Y. Acad. Sci.* **1949**, *51*, 627.
(27) Eppenga, R.; Frenkel, D. *Mol. Phys.* **52**, *52*, 1303.
(28) Fushiki, M. *J. Chem. Phys.* **1992**, *97*, 6700.
(29) Pellenq, R. J. M.; Caillol, J. M.; Delville, A. *J. Chem. Phys. B* **1997**, *101*, 8584.
(30) Larsen, A. E.; Grier, D. G. *Nature* **1997**, *385*, 230.
(31) Thompson, D. W.; Butterworth, J. T. *J. Colloid Interface Sci.* **1992**, *151*, 236.
(32) Avery, R. G.; Ramsay, J. D. F. *J. Colloid Interface Sci.* **1986**, *109*, 448.
(33) Hummer, G. *Chem. Phys. Lett*. **1995**, *235*, 297.
(34) Israelachvili, J. N. *Intermolecular and Surface Forces*; Academic Press: London, 1985.
(35) Löwen, H.; Madden, P.; Hansen, J. P. *Phys. Rev. Lett.* **1992**, *68*, 1081.
(36) Löwen, H.; Hansen, J. P.; Madden, P. *J. Chem. Phys.* **1993**, *98*, 3275.
(37) van Roij, R.; Dijkstra, M.; Hansen, J. P. *Phys. Rev. E* **1999**, *59*, 2010.
(38) Patra, C. N.; Yethiraj, A. *J. Phys. Chem. B* **1999**, *103*, 6080.
(39) Dubois, M.; Zemb, Th.; Belloni, L.; Delville, A.; Levitz, P.; Setton, R. *J. Chem. Phys.* **1992**, *96*, 2278.
(40) Guldbrand, L.; Jönsson, B.; Wennerström, H.; Linse; P. *J. Chem. Phys.* **1984**, *80*, 2221.
(41) Delville, A.; Gasmi, N.; Pellenq, R. J. M.; Caillol, J. M.; Van Damme, H. *Langmuir* **1998**, *14*, 5077.